C O S T E P – COMPREHENSIVE SUPRATHERMAL AND ENERGETIC PARTICLE ANALYSER

R. MÜLLER-MELLIN, H. KUNOW, V. FLEIßNER, E. PEHLKE,
E. RODE, N. RÖSCHMANN, C. SCHARMBERG and H. SIERKS
Institut für Kernphysik, Universität Kiel, 24118 Kiel, Germany

P. RUSZNYAK, S. MCKENNA-LAWLOR and I. ELENDT
St. Patrick's College, Maynooth, Ireland

J. SEQUEIROS, D. MEZIAT, S. SANCHEZ, J. MEDINA and
L. DEL PERAL
Universidad de Alcala de Henares, 28871 Alcala (Madrid), Spain

M. WITTE
Max-Planck-Institut für Aeronomie, 37189 Katlenburg-Lindau, Germany

and

R. MARSDEN and J. HENRION
Space Science Department, ESTEC, 2200 AG Noordwijk, The Netherlands

Abstract. The COSTEP experiment on SOHO forms part of the CEPAC complex of instruments that will perform studies of the suprathermal and energetic particle populations of solar, interplanetary, and galactic origin. Specifically, the LION and EPHIN instruments are designed to use particle emissions from the Sun for several species (electrons, protons, and helium nuclei) in the energy range 44 keV/particle to > 53 MeV/n as tools to study critical problems in solar physics as well as fundamental problems in space plasma and astrophysics. Scientific goals are presented and a technical description is provided of the two sensors and the common data processing unit. Calibration results are presented which show the ability of LION to separate electrons from protons and the ability of EPHIN to obtain energy spectra and achieve isotope separation for light nuclei. A brief description of mission operations and data products is given.

Key words: solar physics – space plasma physics – solar energetic particles – solar flares – coronal mass ejections

1. Introduction

Two investigator groups among the SOHO experimenters jointly form the COSTEP-ERNE Particle Analyser Collaboration (CEPAC). The Comprehensive Suprathermal and Energetic Particle Analyser (COSTEP) comprises two sensor instruments LION and EPHIN together with the common data processing unit (CDPU), while the Energetic and Relativistic Nuclei and Electron experiment (ERNE) is composed of two sensors LED and HED along with the common Low Voltage Power Converter (LVPC). The contributions of the ERNE consortium are discussed in Torsti et al., 1995. In the present paper we discuss the design of the COSTEP portion of the collabo-
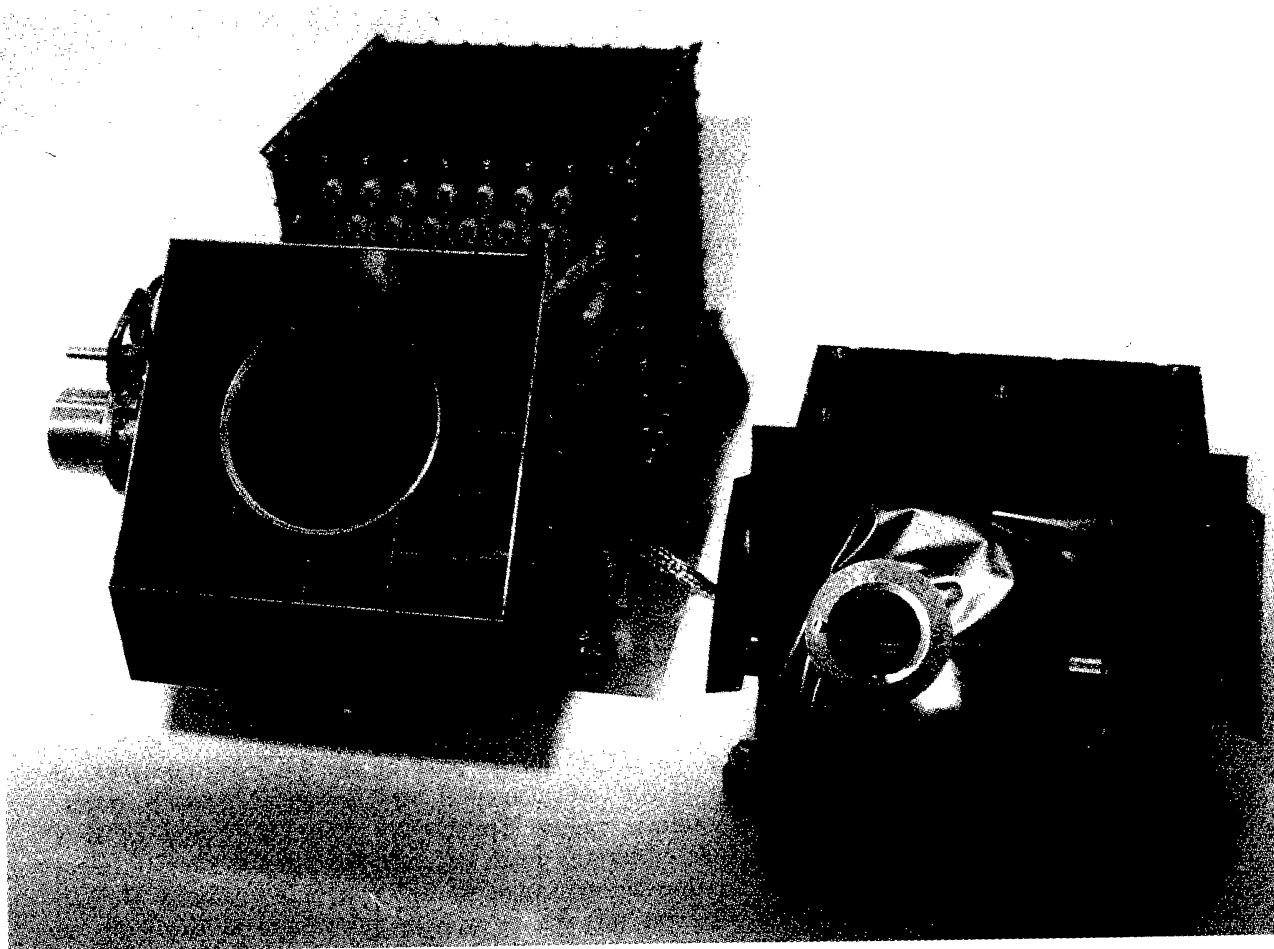
Fig. 1.   COSTEP Sensor Units EPHIN (left) and LION (right)

ration. Additional information can be found in Kunow et al., 1988 and 1992. The COSTEP sensor units are shown in Fig. 1 with EPHIN on the left and LION on the right.

2.   Scientific Goals

COSTEP addresses scientific objectives related to the following phenomena:
  — Steady state processes in the solar atmosphere
  — Energy release and particle acceleration in the solar atmosphere
    · Long duration events
    · Impulsive events
    · Non flare-associated particle events
  — Samples of solar atmospheric material
    · Large solar particle events
    · Elemental abundances of low-Z-elements
    · Isotopic abundances of H and He

· Small, ^{3}He-rich flares and impulsive kilovolt electron events
— Interplanetary medium
 · Travelling shock events
 · Corotating interaction regions
 · Particle propagation in interplanetary space

It is at first surprising that suprathermal and energetic particle emissions, which are generally associated with explosive phenomena, also carry vital information about the quiet solar atmosphere. There are two primary reasons for this. First, continuous emissions of suprathermal electrons (and possibly ions) are associated with processes which operate in the 'quiet' corona. Second, samples of the solar atmosphere accelerated in flares have ionization state temperatures typical of the ambient corona, not the much hotter flare site, and therefore carry information about the ambient coronal composition.

For particles observed in processes with a high energy release, at least four distinct solar acceleration processes have been suggested:
 — Short time scale (impulsive) acceleration related to the flash phase of flares, e.g. from reconnection electric fields.
 — Second order Fermi (stochastic) acceleration in turbulent regions generated by a flare.
 — Low coronal shock acceleration immediately after the impulsive phase, sometimes operating in closed magnetic loops.
 — High coronal shocks associated with the largest (gradual) events and with CME's.

Identification of different acceleration processes requires use of the full range of electromagnetic signatures including radio, optical, UV, X-ray and gammray, along with particle information from suprathermal through the energetic particle range. In the past, only a subset of these diagnostics was available at any one time, making it difficult to synthesize a coherent picture. With SOHO we have for the first time the exciting opportunity to routinely observe particle events using many of these information channels simultaneously.

Acceleration of energetic particles continues in the interplanetary medium, most often associated with shocks and other disturbances. Travelling shocks in the interplanetary medium are produced by various types of solar activity including large flares and CME's. Corotating interaction regions (CIR) are typically observed for several years around solar minimum, when the polar coronal holes expand to the equator, and fast solar wind overtakes the slower wind ahead of it forming a compression region of high magnetic field strength and plasma density. The SOHO primary mission coincides with the minimum of solar activity.

The COSTEP sensors LION and EPHIN will allow a systematic investigation of these questions to be made by measuring energetic particles over

a wide range of energies and for different particle species and combining this information with simultaneous observations from other experiments in the SOHO payload, on other satellites and with ground based observations. Key contributions towards solving these problems can be expected from suprathermal and energetic particle observations, by using these particles as diagnostic tools for remote probing of solar processes. It is possible to distinguish a rich variety of solar phenomena by observing the energetic particles that they emit. Impulsive flares, coronal mass ejections (CME's), disappearing filament events, and interplanetary shock waves, each have as distinctive a signature in the timing, composition, and spectra of the accelerated particles as they do in the radio, optical, X-ray and gamma-ray photons that they produce.

3. Low Energy Ion and Electron Instrument (LION)

3.1 LION SENSOR

LION is a stack of semiconductor detectors to measure energetic particles. The instrument consists of two sensor heads, each containing a double telescope, which together provide the capability to measure particle spectra in the range 44 keV to 6 MeV for protons and 44 keV to 300 keV for electrons (see Table I). A channel for $Z > 1$ particles, mainly alphas in the range 7–26 MeV, is also provided. Count rates are accumulated with 15 s time resolution. Fig. 2 shows one of the two LION sensors consisting of three ion-

TABLE I

LION Data Channels

LION 1 Channels	LION 2 Channels	Energy Range
P1 + E1	P1	44 – 80 keV
P2 + E2	P2	80 – 125 keV
P3 + E3	P3	125 – 200 keV
P4 + E4	P4	200 – 300 keV
P5	P5	300 – 750 keV
P6	P6	0.75 – 2 MeV
P7	P7	2 – 6 MeV
H1 (alphas)	H1	7 – 26 MeV

implanted silicon detectors arranged in a '2 in 1' telescope configuration. On the top are shown two schematic views - rotated through 90° - of the aperture, the deflection magnets, and the detector stack, while on the bottom a perspective view of the detector stack is given. Square ($12 \times 12 \ mm^2$) detec-
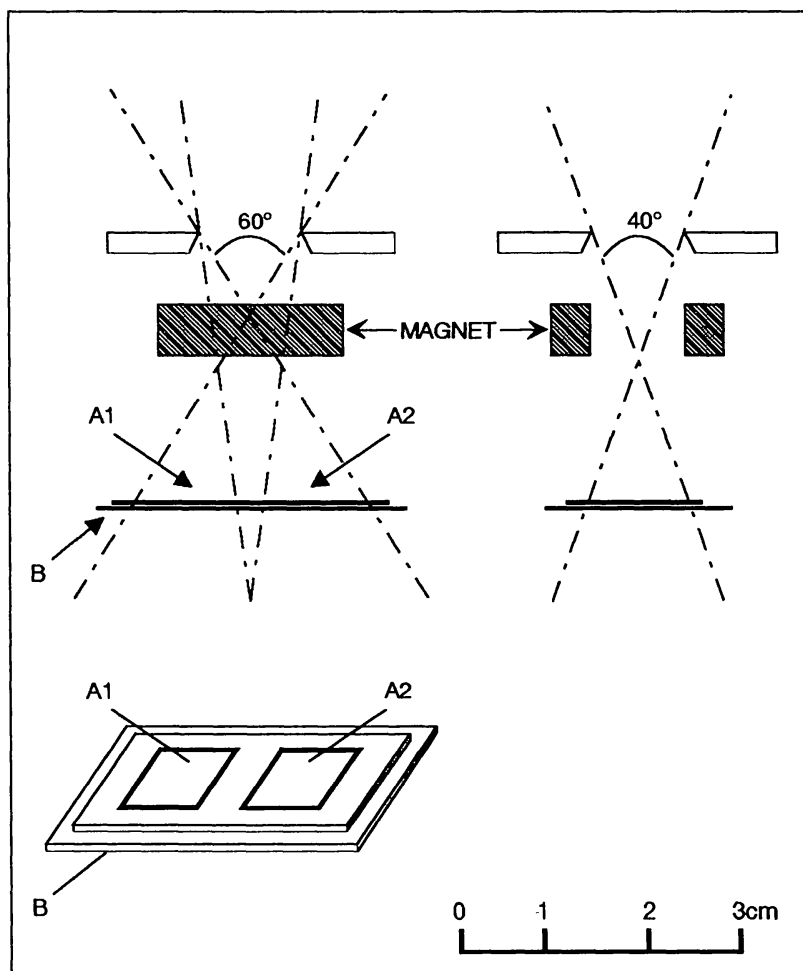
Fig. 2.   LION telescope 2 schematics, top: two views of the aperture, the deflection magnets, and the detector stack - rotated through 90°, bottom: perspective view of the detector stack. Telescope 1 (not shown) without magnet, otherwise identical.

tors A1 and A2 form the dual front elements, making back-to-back contact to the rectangular rear element B (19×34 mm^2). Detector B is operated in anticoincidence to reduce background from penetrating particles. A1 and A2 view the same rectangular entrance aperture, providing a total field of view of $60° \times 40°$ and a total geometric factor of 0.32 cm^2 sr. Each A detector, in combination with the common B detector, forms a distinct particle telescope, providing extended angular coverage for a minimum weight penalty. The LION 2 sensor head employs a 'broom magnet', utilizing rare earth NdFeB material to sweep electrons of energies up to at least 300 keV away from both A detectors. In order to eliminate stray magnetic fields, the magnet has a closed soft iron yoke. Higher energy electrons penetrate

the A detector and trigger the B detector, thereby enabling their separation from higher energy ions. The LION 1 sensor which is identical, except that no broom magnet is included, measures the sum of electrons and protons, thereby enabling the determination by subtraction of electron rates in the energy range below 300 keV.

Both LION sensor heads and their associated electronics are packed into one housing, having envelope dimensions $18.2 \times 15.0 \times 13.3$ cm^3. A sunshade protects the sensor apertures from direct illumination and from stray light. The entrance aperture points in the direction of the nominal interplanetary magnetic field at 1 AU, 45° west of the spacecraft-sun line. The instrument has a total power requirement of 0.9 W; a mass of 2.2 kg and requires a telemetry rate of 40 bits per second.

3.2 LION PROCESSING ELECTRONICS

The LION analog processing electronics consists of two identical sensor interfaces and a section which performs common functions. The signals of particles that have stopped in one of the 4 front detectors are processed in separate analog chains consisting of two-stage-amplifiers and discriminators. The dynamic range extends from 44 keV to 26 MeV, which is divided into 8 energy bins for counting.

The part common to both sensors contains a flight test generator to produce test pulses for periodic checking of the analog signal processing chains; a telecommand decoder/buffer to receive and store commands controlling instrument status; an analog housekeeping monitor to select and convert monitored parameters into digital data, and a detector bias voltage supply. A functional block diagram of the instrument is presented in Fig. 3.

3.3 LION CALIBRATION

The discriminator thresholds were calibrated with radioactive sources: Cd-109 (electrons 62.2 and 84.2 keV), Ba-133 (electrons 238, 266, 319, 349 keV), Bi-207 (electrons 482, 554, 972, 1044 keV), and Am-241 (alphas 5.48 MeV). These provide a good coverage of the LION energy range with well known particle energies, which allowed a precise measurement and adjustment of the thresholds to be made. Special care was taken to match the thresholds of corresponding channels of the sensor with and without magnet in the low-energy range where electron and proton separation is achieved by subtraction. The thresholds for those detectors, which have geometrically the same viewing angle, were adjusted within 1% of the absolute energy value. Table II shows the threshold measurements for the four telescopes, T1 without magnet, T2 with magnet (B=0.3 T), each one containing two detectors D1 and D2.

The behaviour of electrons in the two different sensors of the LION instrument was investigated with electron sources using a special collimator. The
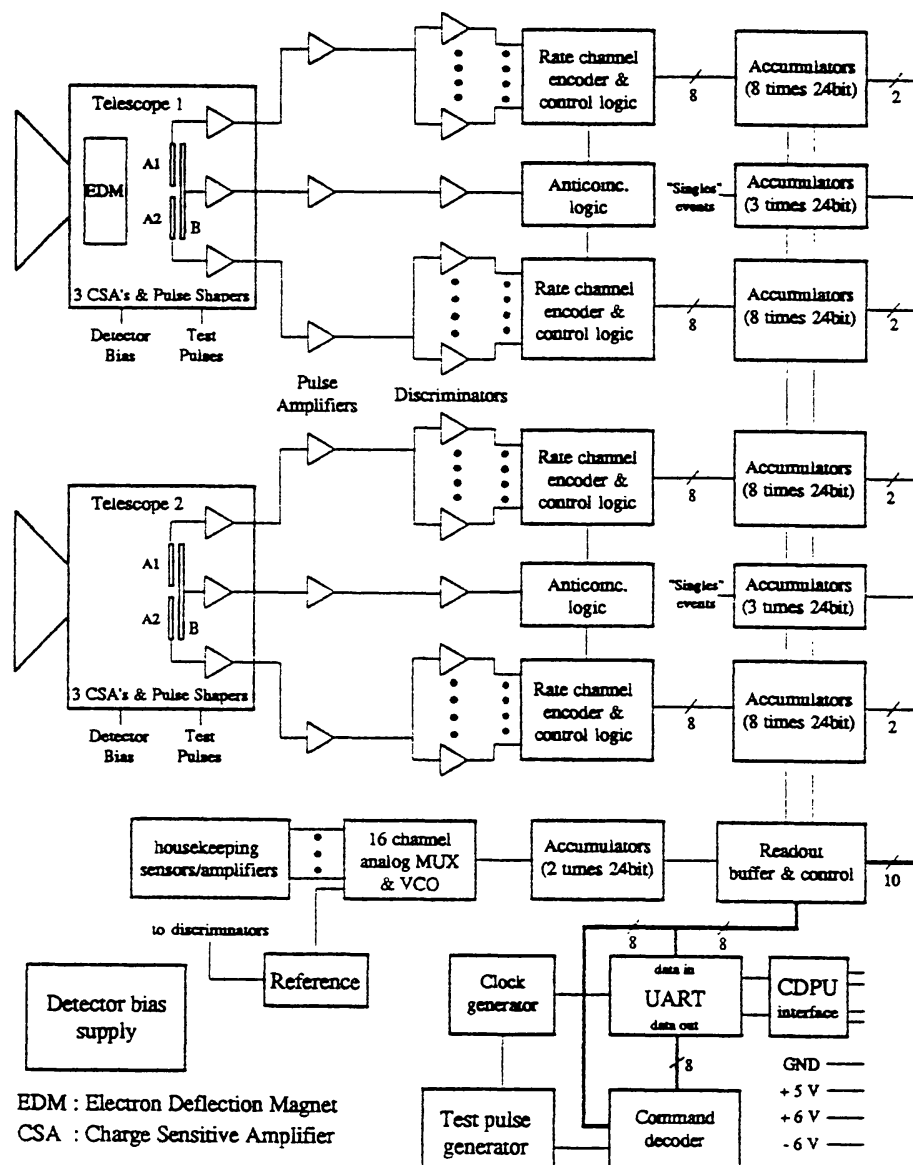
Fig. 3.   LION Functional Diagram

energy loss of electrons in the detectors of the magnetic and non-magnetic sensor were measured as a function of position and incident angle. The results will be analysed and compared with Monte Carlo simulations.

Linearity measurements yielded for each of the eight amplifiers nonlinearities of better than 1% in the energy ranges 44 to 307 keV and 0.76 to 6.8 MeV, respectively. The high-gain amplifiers are driven into saturation at about 18 MeV. The highest energy channel, starting at approx. 6.8 MeV,

TABLE II

LION threshold calibration

T1D1	Energy Range	T2D1	Energy Range
P1 + E1	44.5 - 81.9 keV	P1	44.4 - 81.9 keV
P2 + E2	81.9 - 128.1 keV	P2	81.9 - 128.1 keV
P3 + E3	128.1 - 189.1 keV	P3	128.1 - 190.1 keV
P4 + E4	189.1 - 308.9 keV	P4	190.1 - 309.1 keV
P5	308.9 - 755 keV	P5	309.1 - 754 keV
P6	0.755 - 1.99 MeV	P6	0.754 - 1.96 MeV
P7	1.99 - 6.04 MeV	P7	1.96 - 6.07 MeV
H1	6.87 - 26 MeV	H1	6.87 - 26 MeV

T1D2	Energy Range	T2D2	Energy Range
P1 + E1	44.6 - 81.9 keV	P1	44.6 - 82.0 keV
P2 + E2	81.9 - 127.4 keV	P2	82.0 - 128.2 keV
P3 + E3	127.4 - 193.5 keV	P3	128.2 - 193.9 keV
P4 + E4	193.5 - 305.5 keV	P4	193.9 - 306.1 keV
P5	305.5 - 762 keV	P5	306.1 - 762 keV
P6	0.762 - 2.02 MeV	P6	0.762 - 1.97 MeV
P7	2.02 - 6.02 MeV	P7	1.97 - 6.01 MeV
H1	6.81 - 26 MeV	H1	6.85 - 26 MeV

collects $Z > 1$ particles, mainly alphas. For alpha particles the maximum energy loss in the front detector is 26 MeV at a maximum incident angle of 30°.

4. Electron Proton Helium Instrument (EPHIN)

The EPHIN sensor is a multi-element array of solid state detectors with anticoincidence to measure energy spectra of electrons in the range 250 keV to > 8.7 MeV, and of hydrogen and helium isotopes in the range 4 MeV/n to > 53 MeV/n. The associated signal processing electronics is housed in a separate unit. The units are interconnected by 22 double screened cables. Together, the two units have envelope dimensions of 35.5 x 21.9 x 19.1 cm³. The total mass of EPHIN is 3.55 kg, the total power consumption is 1.85 W and the telemetry rate after onboard data compression is 172 bits per second. The sensor aperture points in the direction of the nominal interplanetary magnetic field at 1 AU, 45° west of the spacecraft Sun line.

Table III summarizes the scientific counting rate channels. Separation of particle species is provided by a set of thresholds also indicated in Table III.

TABLE III

EPHIN Coincidence Channels and Coincidence Conditions

Type	Name	Energy Range				M[1]	P[2]	Coincidence Condition[3]
Electron	E150	0.25	–	0.70	MeV	1	4	A0 $\overline{A1}$ B0 $\overline{C0}$ $\overline{D0}$ $\overline{E0}$ $\overline{F0}$ $\overline{G0}$
	E300	0.67	–	3.00	MeV	1	4	A0 $\overline{A1}$ B0 C0 $\overline{D0}$ $\overline{E0}$ $\overline{F0}$ $\overline{G0}$
	E1300	2.64	–	6.18	MeV	1	4	A0 $\overline{A1}$ B0 C0 D0 $\overline{E0}$ $\overline{F0}$ $\overline{G0}$
	E3000	4.80	–	10.4	MeV	1	4	A0 $\overline{A1}$ B0 C0 D0 E0 $\overline{F0}$ $\overline{G0}$
Proton	P4	4.3	–	7.8	MeV	3	4	A1 $\overline{A4}$ B0 $\overline{C0}$ $\overline{D0}$ $\overline{E0}$ $\overline{F0}$ $\overline{G0}$
	P8	7.8	–	25.0	MeV	3	4	A1 $\overline{A3}$ B0 C0 $\overline{D0}$ $\overline{E0}$ $\overline{F0}$ $\overline{G0}$
	P25	25.0	–	40.9	MeV	3	4	A1 $\overline{A2}$ B0 C0 D0 $\overline{E0}$ $\overline{F0}$ $\overline{G0}$
	P41	40.9	–	53.0	MeV	3	4	A1 $\overline{A2}$ B0 C0 D0 E0 $\overline{F0}$ $\overline{G0}$
Helium	H4	4.3	–	7.8	MeV/N	4	40	A4 B0 $\overline{C0}$ $\overline{D0}$ $\overline{E0}$ $\overline{F0}$ $\overline{G0}$
	H8	7.8	–	25.0	MeV/N	4	16	A3 B0 C0 $\overline{D0}$ $\overline{E0}$ $\overline{F0}$ $\overline{G0}$
	H25	25.0	–	40.9	MeV/N	4	4	A2 B0 C0 D0 $\overline{E0}$ $\overline{F0}$ $\overline{G0}$
	H41	40.9	–	53.0	MeV/N	4	4	A2 B0 C0 D0 E0 $\overline{F0}$ $\overline{G0}$
Integral		E	>	8.70	MeV			
	INT	P	>	53.0	MeV	1	0	A0 B0 C0 D0 E0 F0 $\overline{G0}$
		H	>	53.0	MeV/N			

[1]Multiplicity [2]Priority Buffer Depth [3]Segment index for A and B detector not shown

Note:

(i). 33 coincidence countrates + 17 single detector countrates + 6 calibration/control channels A0n B0n C0 D0 E0 F0 ($n = 0\ldots 5$), total of 56 counters

(ii). thresholds:

A0n =	30 keV	B0n =	60 keV	$n = 0\ldots 5$
A1 =	270 keV	C0 =	370 keV	
A2 =	970 keV	D0 =	580 keV	
A3 =	2.1 MeV	E0 =	580 keV	
A4 =	5.3 MeV	F0 =	150 keV	
		G0 =	100 keV	

4.1 EPHIN Sensor Unit

The heart of the EPHIN sensor head consists of a stack of five silicon detectors, surrounded by an anticoincidence shield of plastic scintillator and a sixth silicon detector to distinguish between absorption and penetration mode (see Fig. 4). Two passivated ion-implanted detectors (A and B) define the 83° full width conical field of view with a geometric factor of 5.1 cm² sr. Detectors A and B are divided into six segments. This coarse position sensing permits sufficient correction for path length variations (resulting
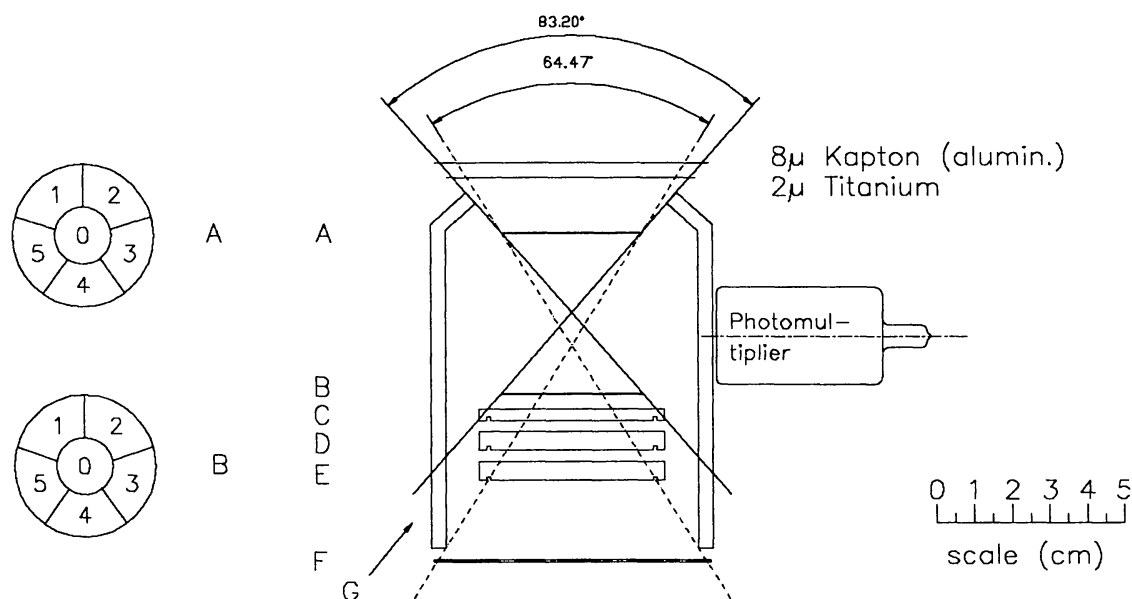
Fig. 4.   Schematic view of the EPHIN sensor. Detail of segmented detectors A and B is shown on left.

from the large field of view) needed to resolve isotopes of hydrogen and helium. Another important advantage of segmentation is the capability to implement a commandable or self-adaptive geometric factor. On detection of high count rates in the centre segment A0 the logic will disable all but the inner circular segments of both detectors A and B, reducing the effective geometric factor by a factor of 24 to permit measurements of fluxes as high as 10^6 counts/(cm^2 s sr) without significant dead time losses.

The lithium-drifted silicon detectors C, D, and E stop electrons up to 10 MeV and hydrogen and helium nuclei up to 53 MeV/N. These large area detectors have thickness variations of less than 10 μm and diffused lithium contact dead layers of less than 50 μm silicon equivalent. The ion-implanted detector F will allow particles stopping in the telescope to be distinguished from penetrating particles. The fast plastic scintillation detector G, viewed by a 1 inch photomultiplier and used in anticoincidence, helps to reduce background. The whole stack is mounted in an aluminium housing, the aperture being covered by two thin foils. The inner titanium foil of 2 μm thickness ensures light tightness and closes the electrical shielding of the sensor while the outer aluminized kapton foil of 8 μm thickness is necessary for thermal control. The detector specifications are given in Table IV.

4.2   EPHIN Electronics

The design of the onboard signal processing electronics is devided into 3 functional groups: the Analog Control Unit (ACU), the Digital Control Unit

TABLE IV

Detector Specifications

Detector	A	B	C	D,E	F
Type	ion-implanted	ion-implanted	Lithium-drifted	Lithium-drifted	ion-implanted
Thickness [μm]	150±10	300±15	3000±10	5000±10	700±15
Active Area [mm^2]	1130	1130	1500	1500	5000
Number of Segments	6	6	1	1	1
α-Res. keV FWHM	36	36	≤150	≤150	80
β-Res. keV FWHM	12	12	–	–	70
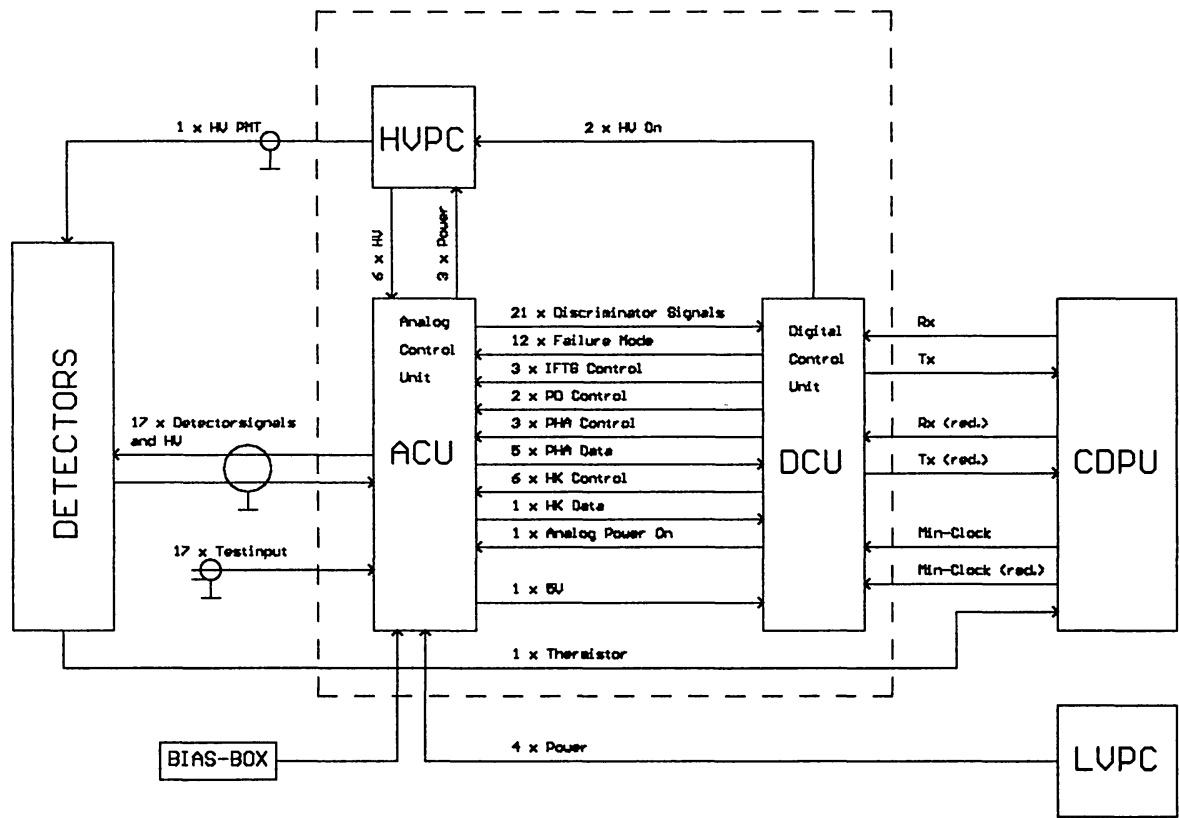
Fig. 5.   EPHIN Electronics Block Diagram

(DCU), and the High Voltage Power Converter (HVPC). A block diagram
is shown in Fig. 5.

Analog Control Unit.   The purpose of the ACU is to amplify the
small charge pulses from 16 semiconductor detectors and a photomultipli-
er and to convert them for the digital processing (see Fig. 6). Each of the

16 semiconductor detector signals is capacitively coupled to a dedicated charge sensitive amplifier (CSA) followed by a pole-zero filter (PZ) and then amplified by two serial amplifiers with a common base line restorer. These high gain signals can trigger a discriminator for counting single detector events and coincidence events. To improve the accuracy while allowing a high dynamic range for the input signals (i.e. $\approx$ 60 dB for the A- and B-channels) both the low-gain and the high-gain amplifier outputs are used for peak detection and 10-bit analog-digital conversion. To reduce the amount of ADC's the 12 amplified signals from the segmented A- and B-detectors are fed into 'Analog-Or Amplifiers' (AOA), whose outputs will follow the highest input level. Additionally the outputs of the A-detector AOA's are connected to four discriminators with higher thresholds that are used to separate electrons, protons and helium nuclei. The photomultiplier tube signal is capacitively coupled to a combined charge sensitive preamplifier, discriminator and pulse shaper. It is used as a veto-signal and is not pulse height analyzed.

Not shown in the ACU scheme is the housekeeping circuitry and the inflight test pulse generator (IFTG). The following 16 physical quantities are A/D-converted to 8-bit housekeeping values:
  - 4 power rail voltages
  - 4 power rail currents
  - 6 leakage currents of A − F detectors,
  - 1 high voltage of photomultiplier tube
  - 1 temperature inside EPHIN electronics box.
In addition a spacecraft powered thermistor is used to record the temperature history of the sensor also when CEPAC is switched off.

For inflight calibration each of the 17 analog channels can be stimulated by generating a charge at the CSA test inputs. There is a predefined sequence of test pulses controlled by the onboard software. Sequence and charge amplitudes can be changed by software upload.

Digital Control Unit. The DCU processes the ACU discriminator signals and A/D conversion results and generates a scientific and a housekeeping data block for transfer to the CDPU once per minute. The DCU also accepts telecommands from the CDPU to control the instrument. The first trigger of an ACU discriminator starts a 2.5 μs coincidence window, during which discriminator signals may set their associated flipflops. At the end of this window the DCU evaluates the coincidence configuration by hardware logic and increments the associated counters. In case of a valid coincidence the DCU starts the pulse height analysis, if the PHA circuitry is not busy with a previous analysis.

There are 56 24-bit counters (see Table III). The column 'M' in Table III indicates the multiplicity of counters, i.e. protons are counted in 3 different counters depending on the position in A and B detectors and incident angle
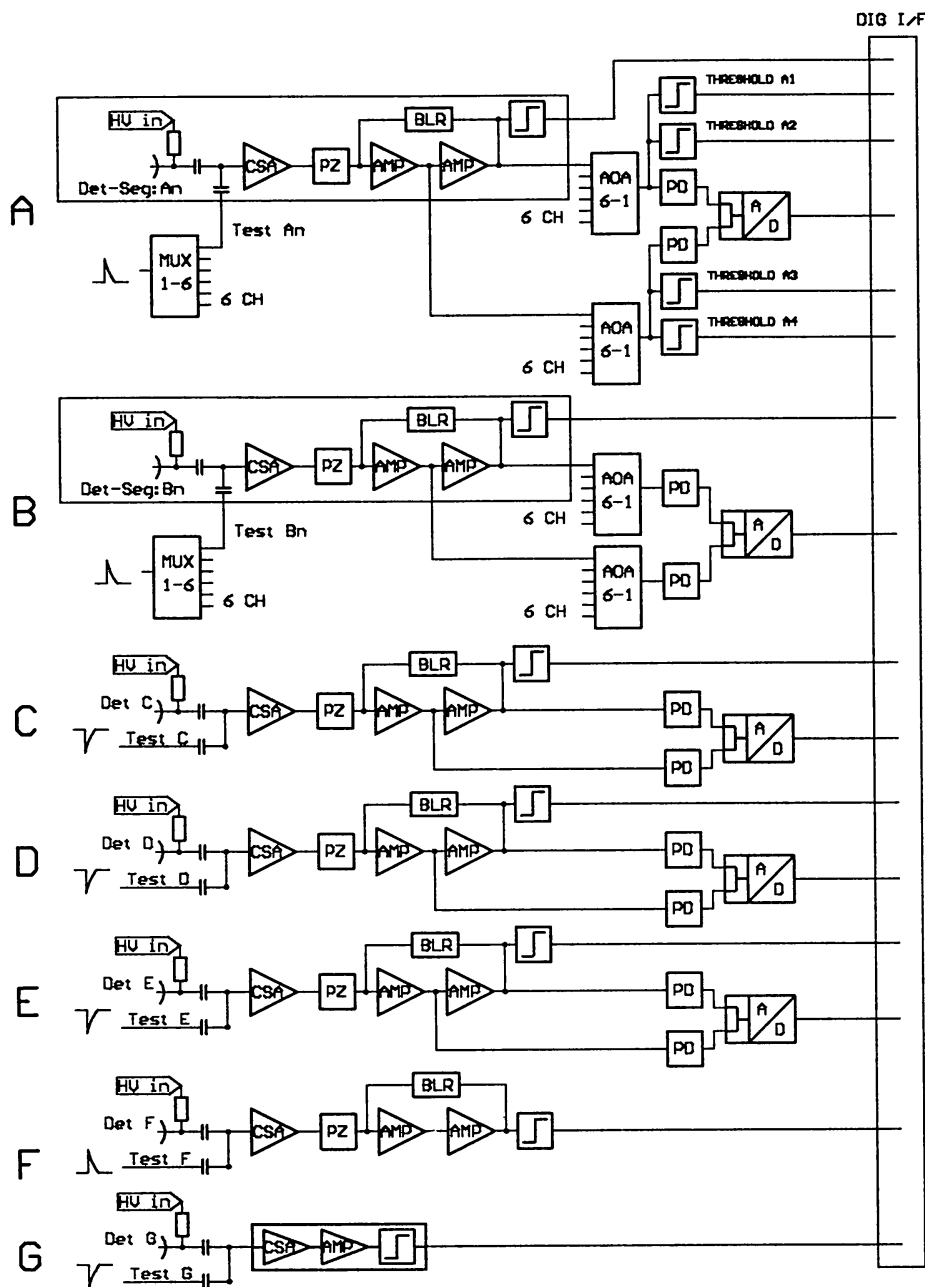
Fig. 6. EPHIN Analog Electronics Block Diagram

of particles: straight in the center sectors A0 B0, straight in the ring sectors An Bn; n=1...5, or oblique, i.e. all other sector combinations. Helium nuclei are counted in 4 different counters similar to protons, whereby the oblique incidence is further distinguished in slightly oblique and strongly oblique. This is needed for ^3He - ^4He separation.

The EPHIN instrument produces 1290 bytes of scientific data during a 1-minute accumulation interval . In order to adjust to higher data rates,

the frame length can be changed in steps of 2 bytes up to 2000 bytes by telecommand. Thus more pulse height information can be transmitted in case bitrate is freed by other instruments within CEPAC.

The data frame is organized in 4 different groups: digital housekeeping, countrates, histograms, and pulse height data.

Digital Housekeeping: 7 bytes at the beginning of the scientific data block are reserved for status information. These bytes contain operational mode, power status, error flags, status of failure mode registers, and a pointer to separate the pulse height data registered in priority mode from those in normal mode.

Countrates: The 24-bit counters are compressed using a $8 + 4$ bit logarithmic compression which allows a decompression with an accuracy better than the statistical accuracy.

Histograms: Histograms provide more detailed spectral information than the countrates though less detailed than the full PHA information. No isotope information can be obtained from the histograms. Histograms are constructed from the pulse height words (PHW) by adding up the energy losses measured in all involved detectors and counting the number of particles versus total energy loss in 64 bins. This is performed separately for the ranges AB, ABC, ABCD, and ABCDE with a time resolution of 8 minutes. Thus only 48 bytes per minute are reserved for compressed (8+4) histogram information. This onboard processing provides spectral information for electrons, protons, and helium at a marginal bitrate increase.

Pulse Height Data: In normal observation mode the PHW buffer of 1151 bytes is filled with PHW's in chronological order. A PHW is composed of a 10 bit header and two or more A/D conversion results.The header consists of 3 bits each for the sector information of detectors A and B, and 4 bits to hold the coincidence type. 11 bits are added for each involved channel A, B, C, D, and E: 10 bits with the ADC result and 1 bit that indicates the gain range. Depending on the coincidence depth the size of PHW's can vary between 4 and 9 bytes. If the PHW buffer is filled before the accumulation period ends, the buffer is overwritten in reverse direction starting at the end address with priority pulse height data. The priority system is designed to assure transmission of a minimum number of events per sampling intervals for each particle type and energy range when the PHW buffer is flooded by overabundant particles. This minimum number which is indicated in column 'P' in Table III is initialized in the EPHIN onboard software, but can be changed by table upload.

High Voltage Power Converter.   For biasing the semiconductor detectors A to F and for operating the photomultiplier tube G there are 7 individually adjustable high voltages provided by 3 independently regulated HV cascades: A (-30 V), B (-60 V), C (+400 V), D (+600 V), E (+600 V), F (-140 V), and G (+900 V). The converter frequency is 64 kHz.
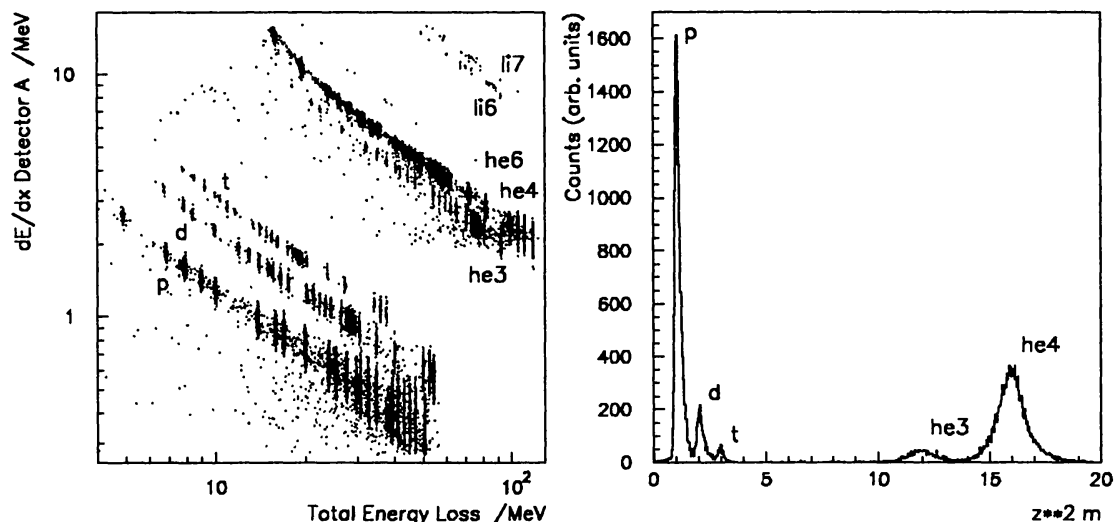
Fig. 7. *left* : Mass separation of p, d, t, and ^{3}He, ^{4}He achieved at HMI/Berlin cyclotron with 120 MeV ^{4}He primary beam on Au-target. A minor population of ^{6}He, ^{6}Li, and ^{7}Li can be identified. *right* : Mass separation $z^2 \cdot m$ resolved via projection of HMI results along theoretical energy-loss curves.

4.3 EPHIN CALIBRATION

The semiconductor detectors A-F have been calibrated individually using an ^{241}Am source resulting in a single-point calibration of the detector/electronics system and the onboard data analysis.

The scintillator-photomultiplier combination of the anticoincidence detector G has been calibrated in terms of photoelectron production for minimum-ionising particles using a ^{207}Bi source and cosmic-ray muons. Due to the shape of the detector, the light collection is position dependent. Worst case analysis shows a signal well above detection threshold.

Cosmic-ray muons and air shower electrons have been used to gather information about long-term variations of the detector performance while the instrument is still on ground. Instrument resolution for cosmic-ray muons is 18 keV in detectors An, 25 keV in Bn, 200 keV in C, 340 keV in D and E (FWHM).

The EPHIN calibration with hydrogen and helium nuclei was done with the facilities and support of the Hahn-Meitner-Institut in Berlin/Germany. The desired low energies (4-120 MeV) and low intensities (~100 cps) were realized by using the reaction products from the interaction of the primary 120 MeV ^{4}He beam with a gold target. By means of a magnet spectrometer and a small slit in the focal plane it was possible to select particles of a certain magnetic rigidity with an energy resolution of better than 0.5%. The instrument was positioned in the vacuum chamber as close as possible to the slit, while still leaving enough space for linear and angular displacement of the sensor. Fig. 7 demonstrates the separation of the different nuclei for
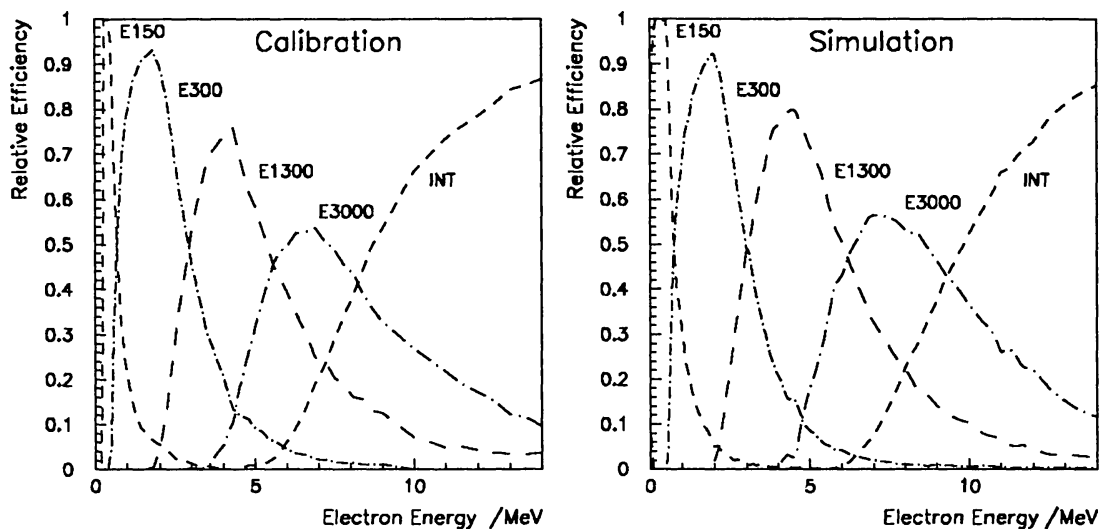
Fig. 8.   Classification of electrons as number of coincidence counts normalized to total number of detected coincidences measured at INW/Gent (*left*) and via Monte-Carlo simulation (*right*).

absorbed particles.

The calibration with electrons was done with the facilities and support of the Nuclear Physics Laboratory INW in Gent/Belgium. Over the full energy range (0.2-14 MeV) the dark current of the linear accelerator produced sufficient intensities. The energy selection was done using an aluminium target and focussing magnets with collimators resulting in an energy resolution of better than 100 keV. The measurements were carried out in vacuum.

The relative efficiencies of the different electron channels compared to the results of a Monte-Carlo Simulation of the instrument are shown in Fig. 8. The energy resolution of 1 MeV electrons (as an example) stopping in detector C is shown in Fig. 9.

The calibration data analysis has not been completed yet. The results will not only yield detailed response and efficiency characteristics of the instrument, but will also be used to verify the mathematical model incorporated in a Monte-Carlo Simulation to analyse the flight data.

5.   THE COMMON DATA PROCESSING UNIT (CDPU)

5.1   DEFINITION AND FUNCTIONS

The data and telecommand interface between the four CEPAC (COSTEP and ERNE) sensors and the SOHO On-Board Data Handling (OBDH) System is provided by a Common Data Processing Unit (CDPU). The CDPU also provides the power rail and power switching interface between the CEPAC Low Voltage Power Converter (LVPC) and the sensors.
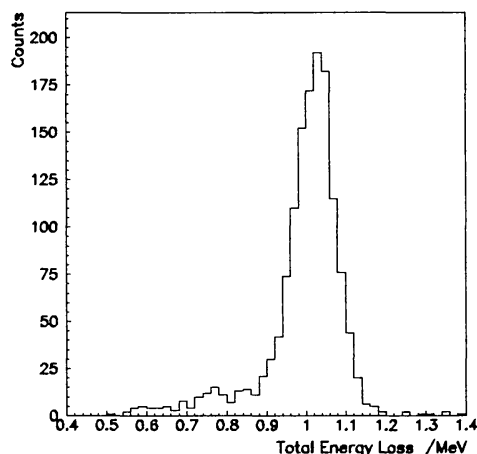
The CDPU main functions are:

Fig. 9.   Energy resolution of 1 MeV electrons stopping in detector C as sum of signals of detectors A, B, and C.

— Request and collect scientific data from the 4 sensors periodically by polling, with time-out protection, and capability of change of the polling scheme by telecommand.
— Request and collect housekeeping data from the 4 sensors, LVPC and CDPU itself periodically.
— Reduce data redundancy for non-intelligent LION sensor.
— Time tag data.
— Format data for transmission by the spacecraft telemetry system.
— Accept, syntactically check and distribute commands to the 4 sensors. Execute commands addressed to itself.
— Accept and distribute control tables and software, sent from ground station to intelligent sensors HED, LED, and EPHIN.

5.2   CDPU ARCHITECTURE

To increase the overall reliability of the CEPAC instrument, the CDPU is composed of two complete and identical 'cold redundant' subunits, each subunit made up of two multilayer (12 layer each) polyimide printed circuit boards with components on both sides. The CDPU has three types of redundant interfaces: with the spacecraft OBDH, with the CEPAC sensors, and with the power converter (LVPC) (see Fig. 10).

5.3   CDPU DESIGN FEATURE

The kernel of the CDPU is the MARCONI MAS281 16-bit microprocessor, manufactured in CMOS Silicon on Sapphire (SOS) technology, radiation resistant up to 100 krads, very low single even upset rate and latch-up free. This microprocessor also complies with the MIL-STD-1750A standard, which provides a good software development environment. Due to power
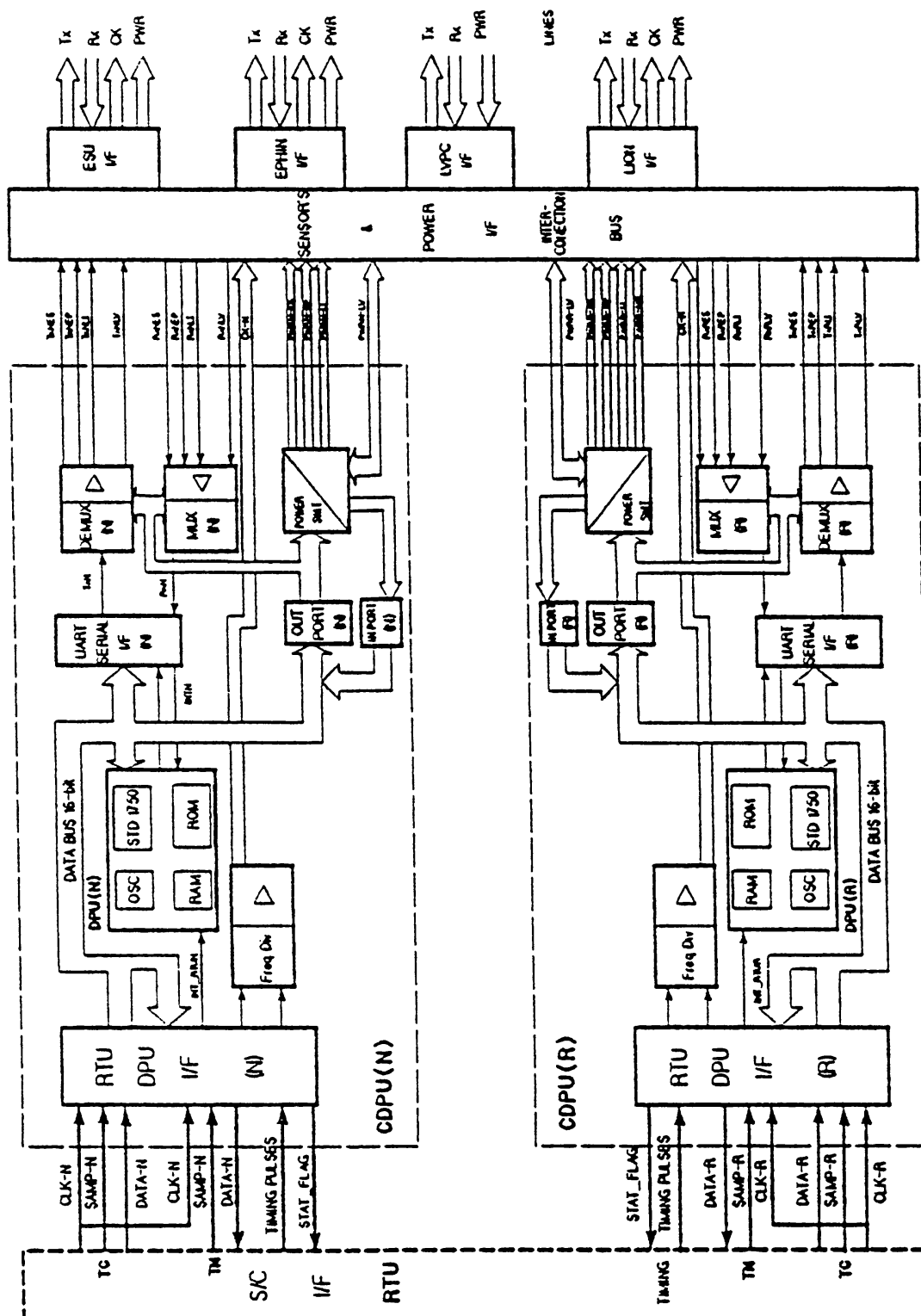
Fig. 10.   CDPU Block Diagram

limitation and low bit-rate requirement, an operating frequency of 5 MHz is chosen.

The 32 kbyte ROM is of bipolar type to avoid latch-up or SEU effects.

Due to the high power consumption of this type of memory, their contents is transferred to CMOS SOS MA6116 RAM after switch-on for program execution and the ROM is switched off. Scientific and housekeeping data are buffered in 16 kbyte of CMOS SOS RAM.

The communication with sensors and LVPC is based on a bidirectional serial asynchronous line Marconi MA28151 UART also in SOS technology. The communication rate is 9600 bps. The selection of sensor communication lines is performed by a MUX-DEMUX function and front-end line buffers-drivers. The total power consumption in nominal operation is 1.6 W. The total mass of the unit, which is of about 245x204x88 mm^3 in dimension and an average wall thickness of 0.8 mm, is less than 2.4 kg.

The software is written almost exclusively in ADA language. Only those functions which require a critical execution time are written in assembly language. The communication protocol between the CDPU and the intelligent sensors is based on a simplified version of ANSI X3.28.

6.   COSTEP mission operations

Five days after launch, when SOHO is in its transfer trajectory phase (TTP), the COSTEP instruments will be switched on. They are designed to operate continuously in nominal observation mode. This mode is only interrupted

— to perform a comprehensive functional checkout, called commissioning, around day 12 into the mission,
— to go into a safe mode during the midcourse correction manoeuver (MCC2), around day 20 into the mission,
— and about once per month to command EPHIN and LION into calibration mode for a duration of less than 1 hour.

The instruments can be reconfigured in order to recover from possible failures. The following telecommands are used to operate the EPHIN and LION instruments during ground testing and in space:

— EPHIN reset
— load EPHIN failure mode register 1 (generates $\overline{A0n}$ or A00 or disables/enables automatic geometric factor switching)
— load EPHIN failure mode register 2 (generates $\overline{B0n}$ or B00)
— load EPHIN failure mode register 3 (generates C or D or E or $\overline{F}$ or $\overline{G}$)
— load EPHIN power register (switch on/off analogue power, detector bias, phototube high voltage)
— define EPHIN mode (standby, nominal observation, calibration)
— upload EPHIN memory (tables or program patch)
— download EPHIN memory (tables or program)
— LION reset
— define LION mode (nominal observation, calibration)
— switch LION threshold (low, high level)

— enable/inhibit LION internal current limiter

— test LION anticoincidence logic

— CDPU switch sensors on/off (LION, EPHIN, ESU DPU1, ESU DPU2)

— CDPU redistribute telemetry bitrate

— upload CDPU memory (program patches)

— download CDPU memory (program)

Unlike the optical experimenters, the investigators of particle data cannot control where, in the solar corona, their individual instruments are pointing. Since particles travel along magnetic field lines, the point of contact with the Sun is defined by the magnetic field line connecting SOHO with the solar corona. Thus, whatever particles manage to get on to that field line can, in principle, be measured by the onboard particle detectors. Definition of the solar contact area is uncertain by about $\pm 15°$. It is a particular problem that no magnetic measurements are made aboard SOHO itself and that such data must be separately obtained.

The particles measured at the spacecraft have probed both the corona and interplanetary space. Thus, to correctly interpret these records, it is necessary to collect as much information as possible concerning the history of the parent event. In this respect, the optical instruments can identify areas of interest on the Sun for the particle experimenters both before and after particular measurements.

A complication in correlating optical and particle data is the delay between the measurement of particles onboard SOHO and their original time of release from the solar atmosphere. Electrons of high energies travel with velocities approaching a significant fraction of the speed of light, so that they arrive at the spacecraft within minutes after the information provided by the optical instruments. Particles of lower energies, expecially nuclei, require travel times of from hours to days from the Sun to SOHO and this transit time further depends on the prevailing magnetic configuration.

Because of these long delay times, co-ordinated observations between the particle and optical instruments require the definition of extended observation campaigns devoted to the investigation of particular phenomena (e.g. microflares; steady state acceleration processes of suprathermal and energetic particles etc.). More than one feature of interest can, of course, be studied during a particular campaign. The definition of co-ordinated activities will be the subject of formal agreements between the optical and 'in-situ' experimenter teams. Co-operative activity between the particle experimenters and theoreticians modelling various features of the solar atmosphere, will also be formalized.

7. Data Products

COSTEP will produce 20 Megabit of science data and 0.8 Megabit of house-keeping data per day. Starting from real-time and playback level 0 telemetry data, this information will be processed at the home institutes together with ancillary data and synoptic information from other spacecraft, ground based stations, and SOHO summary data. The resulting level 1 COSTEP data is used for further scientific processing and data exchange. The processed data are of the type: intensity-time profiles, abundance ratios, and energy spectra for the species electrons, hydrogen isotopes, and helium isotopes.

The COSTEP contribution to the summary data set, generated daily at the ISTP Central Data Handling Facility (CDHF) and immediately available to the SOHO science community at the Experiment Operations Facility (EOF), consists of 5-minute averages of the counting rates in Table V (Key Parameters).

TABLE V
COSTEP Key Parameters

Channel	Sensor	Species	Energy Range	
E150	EPHIN	electron	0.2 - 0.7	MeV
E300	EPHIN	electron	0.7 - 3.0	MeV
E1300	EPHIN	electron	2.6 - 6.2	MeV
E3000	EPHIN	electron	4.8 - 10.4	MeV
P5	LION	proton	0.3 - 0.8	MeV
P6	LION	proton	0.8 - 2.0	MeV
P7	LION	proton	2.0 - 6.0	MeV
P4	EPHIN	proton	4.3 - 7.8	MeV
P8	EPHIN	proton	7.8 - 25.0	MeV
P25	EPHIN	proton	25.0 - 40.9	MeV
P41	EPHIN	proton	40.9 - 53.0	MeV
H4	EPHIN	helium	4.3 - 7.8	MeV/n
H8	EPHIN	helium	7.8 - 25.0	MeV/n
H25	EPHIN	helium	25.0 - 40.9	MeV/n
H41	EPHIN	helium	40.9 - 53.0	MeV/n

Acknowledgements

References

Kunow, H., Fischer, H., Green, G., Müller-Mellin, R., Wibberenz, G., Holweger, H., Evenson, P., Meyer, J.P., Hasebe, N., von Rosenvinge, T., Reames, D., Medina, J., Witte, M., Matsuoka, M., Marsden, R.G., Sanderson, R.R., Wenzel, K.-P., McKenna-Lawlor, S., Sequeiros, J., Doke, T., and Kikuchi, J.: 1988, 'COSTEP' - Comprehensive Suprathermal and Energetic Particle Analyser for SOHO, in V. Domingo, editor, *The SOHO Mission - Scientific and Technical Aspects of the Instruments*, **ESA SP-1104**, 75 - 80

Kunow, H., Müller-Mellin, R., Sierks, H., McKenna-Lawlor, S., Sequeiros, J.: 1992, - COSTEP- Comprehensive suprathermal and Energetic Particle Analyser for SOHO - Scientific Goals and Data Description, *Proc. First SOHO Workshop*, **ESA SP-348**, 43 - 46

Torsti, J., Valtonen, E., Lumme, M., Peltonen, P., Eronen, T., Louhola, M., Riihonen, E., Schultz, G., Teittinen, M., Ahola, K., Holmlund, C., Kelhä, V., Leppälä, K., Ruuska, P., Strömmer, E.: 1995, Energetic Particle Experiment ERNE, *this issue of Solar Physics*